JOURNAL OF AGRICULTURAL AND FOOD CHEMISTRY

Article

pubs.acs.org/JAFC

Metabolite Profiles of Epimedin B in Rats by Ultraperformance Liquid Chromatography/Quadrupole-Time-of-Flight Mass Spectrometry

Li Cui,[†,‡] E Sun,[†] Zhenhai Zhang,[†] Qian Qian,[†] Xiaobin Tan,[†] Fengjuan Xu,[†] and Xiaobin Jia*[,†]

[†]Key Laboratory of New Drug Delivery System of Chinese Meteria Medica, Jiangsu Provincial Academy of Chinese Medicine, 100 Shizi Road, Nanjing 210028, Jiangsu Province, China

[‡]Nanjing University of Chinese Medicine, Nanjing 210046, Jiangsu Province, China

ABSTRACT: In this work, the metabolite profiles of epimedin B in rat feces, bile, urine, and plasma were qualitatively investigated, and the possible metabolic pathways of epimedin B were subsequently proposed. After oral administration of epimedin B at a single dose of 80 mg/kg, rat biological samples were collected and pretreated by protein precipitation. Then, these pretreated samples were injected into an Acquity ultraperformance liquid chromatography BEH C_{18} column with mobile phase consisting of 0.1% formic acid−water and 0.1% formic acid−acetonitrile and detected by ultraperformance liquid chromatography/quadrupole-time-of-flight mass spectrometry. In all, 43 metabolites were identified in the biosamples. Of these, 13, including **F5**, **F7**, **F16**−**F18**, **D5**−**D7**, **D9**, **N5**, **N7**, **M1**, and **M3**, were to our knowledge reported for the first time. The results indicated that epimedin B was metabolized via desugarization, dehydrogenation, hydrogenation, hydroxylation, demethylation, glucuronidation, and glycosylation pathways in vivo. Specific hydrolysis of 7-*O*-glucosides in the gut lumen and glucuronic acid conjugation in the liver were considered as the main physiologic processes of epimedin B. This study revealed the possible metabolite profiles of epimedin B in rats.

KEYWORDS: *epimedin B, UPLC/Q-TOF-MS, metabolic pathways, metabolites, glucuronic acid conjugation*

INTRODUCTION

Herba Epimedii, the dried aerial parts of *Epimedium* L. (Berberidaceae), has been traditionally used as an aphrodisiac, tonic, and herbal antirheumatic drug for bone loss and cardiovascular and impotence diseases in China for over 2000 years.[1,2] This plant is also cultivated in Japan, Korea, and the Mediterranean region.[3,4]

Prenylflavonoids are reported to be an important class of bioactive ingredients in *Epimedium*. Epimedin B, the principal prenylflavonoid in *Epimedium brevicornum* Maxim, is known to promote the proliferation of osteoblast-like cells and has potential activity against osteoporosis.[2,5] These biological activities stimulated us to investigate the pharmacokinetic characteristics of epimedin B. In our previous study, we had used Caco-2 and rat intestinal perfusion models to assess the oral bioavailability and metabolism of epimedin B in rat intestine.[6] However, the metabolite analysis of epimedin B in biosamples of animal origin has not yet been performed. The metabolite profiles and metabolic pathways of epimedin B need to be determined.

The metabolism of prenylflavonoids has been comprehensively studied using methods such as capillary electrophoresis (CE), gas chromatography/mass spectrometry, and liquid chromatography/mass spectrometry.[7−9] However, because of the limitations of the instrument used in these methods, detecting many trace metabolites was difficult under certain conditions. Hence, animal bioavailability studies on prenylflavonoids are limited. Recent development in chromatographic techniques allowed the in vivo quantitative analyses of prenylflavonoids by using ultraperformance liquid chromatography/quadrupole-time-of-flight mass spectrometry (UPLC/Q-TOF-MS) with automated data analysis (Metabolynx).

In this study, pure epimedin B was orally administrated to rats, and the biosamples were collected and analyzed using UPLC/Q-TOF-MS. In all, 18, 9, 10, and 6 metabolites were identified or tentatively characterized from the feces, bile, urine, and blood, respectively, of rats administered epimedin B. The absorption, metabolism, and excretion of orally administrated epimedin B were comprehensively investigated. In addition, the possible physiological disposing pathway of epimedin B was proposed.

MATERIALS AND METHODS

Chemicals. Epimedin B (purity >98%) was isolated from the aerial parts of *E. brevicornum* Maxim. High-performance liquid chromatography grade acetonitrile and methanol were purchased from Merck (Darmstadt, Germany). MS-grade formic acid was purchased from Nanjing Chemical Reagent Co., Ltd. (Nanjing, China). Deionized water was purified using the Milli-Q water purification system (Millipore, Bedford, MA, USA). All the other reagents and chemicals were of analytical grade.

Animal and Drug Administration. Male Sprague−Dawley rats (250 ± 20 g of body weight) were obtained from SLEK Lab Animal Center (Shanghai, China). Rats used in the metabolism studies were housed in an animal room at an ambient temperature of 22−24 °C and a relative humidity of 60%. Food and water were provided ad libitum. The studies were conducted according to protocols approved by the Animal Ethics Committee of Jiangsu Provincial Academy of Chinese Medicine. A day before the experiment, the rats were fasted overnight but were provided deionized water. The rats were divided into two groups: epimedin B and blank control; each group contained

Received: September 10, 2012
Revised: January 16, 2013
Accepted: January 28, 2013
Published: January 29, 2013

three rats. Epimedin B dissolved in 20% polyethylene glycol 400 was orally administered to the rats at a single dose of 80 mg/kg of body weight.[10] Blank control group rats were orally administered deionized water at a dose of 10 mL/kg of body weight.

Sample Collection. Blood samples (500 μL) obtained via the orbital sinus were collected into heparinized tubes at 15, 30, 45, 60, 90, 120, 240, 420, 600, and 780 min after the administration of epimedin B. Next, the blood samples were centrifuged for 10 min at 3000 rpm, 4 °C, and the supernatants were stored.

For the collection of feces and urine samples, three rats were housed in stainless steel metabolic cages and provided free access to deionized water. Samples were collected at 0−12 h and 12−24 h after epimedin B administration.

For the collection of bile samples, rats were fixed on a wooden plate and anesthetized with 5% urethane. An abdominal incision was made, and the common bile duct was cannulated using PE-10 tubing (i.d. = 0.08 cm, Becton Dickinson, Franklin Lakes, NJ, USA) for the collection of bile samples. Epimedin B was consciously administered to three rats by oral gavage. Bile samples were collected during the 0−12 h period after epimedin B administration.

All the samples were stored at −70 °C until additional extraction and analysis.

Sample Preparation. For precipitation of proteins, the samples were prepared as follows. Briefly, 500 μL, 2 mL, and 1 mL of acetonitrile were added to 200 μL of blood, 1 mL of urine, and 500 μL of bile, respectively. Successively, the mixed samples of blood, urine, and bile were mixed by vortexing for 5 min, followed by centrifugation at 14 000 rpm for 10 min. The supernatants of the samples were transferred to clean test tubes and evaporated to dryness at 40 °C under a gentle stream of nitrogen gas. The residue was reconstituted in 200 μL of initial mobile phase acetonitrile−water (5:95) followed by vortexing and centrifugation at 14 000 rpm for 15 min. Subsequently, 20 μL aliquots of the supernatant were injected into the chromatographic system for analysis.

Feces samples (0.5 g) were mixed in 5 mL of methanol. After ultrasonic extraction for 30 min, the samples were centrifuged at 14 000 rpm for 10 min. Then, a 20 μL aliquot of the supernatant was injected into the UPLC system.

Instrumentation and Conditions. Chromatography was performed using an ACQUITY UPLC system (Waters Corp., Milford, MA, USA) equipped with a conditioned autosampler at 4 °C. The separation was carried out on an Acquity UPLC BEH C_{18} column (i.d., 1.7 μm; 2.1 mm × 50 mm; Waters, Milford, MA, USA). The column temperature was maintained at 35 °C. The mobile phase consisted of 0.1% formic acid−water (solvent A) and 0.1% formic acid−acetonitrile (solvent B). The linear gradient elution program was as follows: 0−4 min, 5−50% B; 4−8 min, 50−100% B; 8−9 min, 100% B; 9−9.5 min, 100−5% B; 9.5−11 min, 5% B. The injection volume was 5 μL.

The high-mass resolution experiments were performed on a Synapt Q-TOF mass spectrometer (Waters, Milford, MA, USA) equipped with an electrospray ionization (ESI) source in the positive ion mode. The capillary and cone voltages were 2000 and 40 V, respectively. The desolvation gas (nitrogen) was set to 700 L/h at 350 °C, and the source temperature was 120 °C. The mass range was scanned from 50 to 1200 Da and corrected during acquisition using an external reference (lock spray) consisting of a solution of 600 ng/mL leucine enkephalin (m/z 566.2771) infused at a rate of 5 μL/min. The transfer collision energy (E_c) and trap E_c to acquire MS data were 4 and 6 eV, respectively, whereas the transfer E_c was 15 eV and the trap E_c was ramped from 25 to 40 eV to acquire MS/MS data. The raw data was acquired and processed by MassLynx (version 4.1; Waters).

RESULTS AND DISCUSSION

The full scan mass spectrum of fragment ions of the biosamples collected from rats treated with epimedin B was compared with that of biosamples collected from control rats to identify the possible metabolites of epimedin B. On the basis of the previous investigation of credible MS and MS/MS fragmentation behaviors of epimedin B, the structures of most metabolites were deduced in the present paper, clarifying the general metabolism of epimedin B in vivo. Relatively abundant amounts of metabolites were detected in the feces, urine, and bile with trace amounts found in the plasma samples. The biotransformation of epimedin B in vivo was determined by speculating the structures of the metabolites on the basis of the metabolism rules of epimedin B and mass spectral fragmentation pathways of prenylflavonoids reported previously.[11,12]

Table 1. Accurate Mass Measurement for the Protonated Molecules of Metabolites in Rat Feces

no.	formula	t_R (min)	calcd m/z	exptl m/z	mg/L error
P	$C_{38}H_{48}O_{19}$	2.82	809.2790	809.2895	3.4
F1	$C_{21}H_{20}O_6$	5.58	369.1260	369.1320	−4.9
F2	$C_{21}H_{18}O_7$	4.89	383.1053	383.1136	1.4
F3	$C_{21}H_{20}O_7$	4.66	385.1209	385.1283	−1.0
F4	$C_{27}H_{28}O_{11}$	3.32	529.1632	529.1699	−2.0
F5	$C_{27}H_{30}O_{12}$	2.96	547.1737	547.1813	−0.4
F6	$C_{31}H_{36}O_{14}$	3.42	633.2105	633.2169	−2.2
F7	$C_{32}H_{34}O_{14}$	3.36	643.6040	643.6100	−0.7
F8	$C_{32}H_{36}O_{14}$	4.48	645.2105	645.2192	1.4
F9	$C_{32}H_{36}O_{14}$	4.52	645.2105	645.2173	−1.6
F10	$C_{32}H_{38}O_{14}$	4.02	647.2262	647.2349	1.5
F11	$C_{32}H_{38}O_{14}$	4.04	647.2262	647.2353	2.1
F12	$C_{32}H_{36}O_{15}$	3.34	661.2054	661.2133	0.1
F13	$C_{32}H_{38}O_{15}$	3.28	663.2211	663.2290	0.2
F14	$C_{32}H_{38}O_{15}$	3.82	663.2211	663.2289	0.0
F15	$C_{33}H_{40}O_{15}$	3.88	677.2367	677.2433	−1.8
F16	$C_{32}H_{38}O_{16}$	2.52	679.2160	679.2251	1.9
F17	$C_{32}H_{38}O_{16}$	2.92	679.2160	679.2241	0.5
F18	$C_{32}H_{40}O_{16}$	2.78	681.2316	681.2381	−2.0

Table 2. Relative Peak Area of Metabolites in Feces of Different Collection Times[a]

no.	0−12 h	12−24 h
P	33.60	11.60
F1	139.60	369.40
F2	9.20	4.89
F3	7.60	32.40
F4	N/A	87.50
F5	7.10	N/A
F6	N/A	11.40
F7	N/A	129.20
F8	55.80	N/A
F9	N/A	86.10
F10	1004.70	N/A
F11	N/A	1497.40
F12	126.80	N/A
F13	139.40	507.50
F14	N/A	1.10
F15	58.00	45.60
F16	2.60	N/A
F17	N/A	132.30
F18	7.50	2.78

[a]N/A = not available.

Metabolites Detected in the Rat Feces Samples. In all, 18 metabolites (**F1**−**F18**) were identified or tentatively characterized by MS in the rat feces (Table 1). Of these, five, including **F5**, **F7**, and **F16**−**F18**, were to our knowledge reported for the first time. The relative peak area of the metabolites detected in the feces at different collection times is

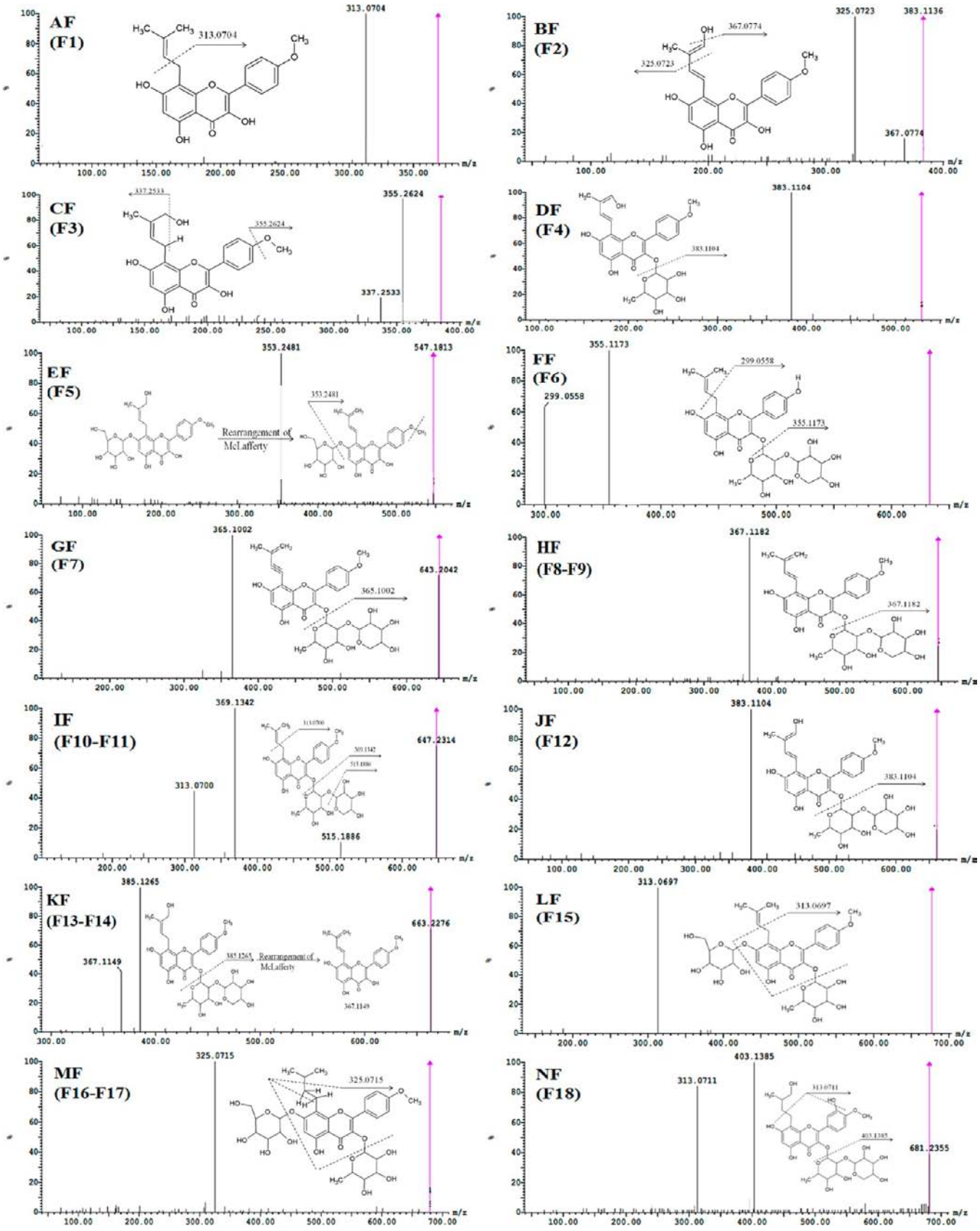

Figure 1. Mass spectra of metabolites of epimedin B in rat feces.

shown in Table 2. The TOF-MS spectra of these metabolites and the proposed major metabolic pathway of epimedin B in rat feces are shown in Figures 1 and 2, respectively.

The molecular ions of **F10** and **F11** (m/z 647.2262), **F15** (m/z 677.2367), and **F1** (m/z 369.1260) were produced by the neutral loss of 162, 132, and 440 Da, corresponding to the

dx.doi.org/10.1021/jf304625x | J. Agric. Food Chem. 2013, 61, 3589−3599

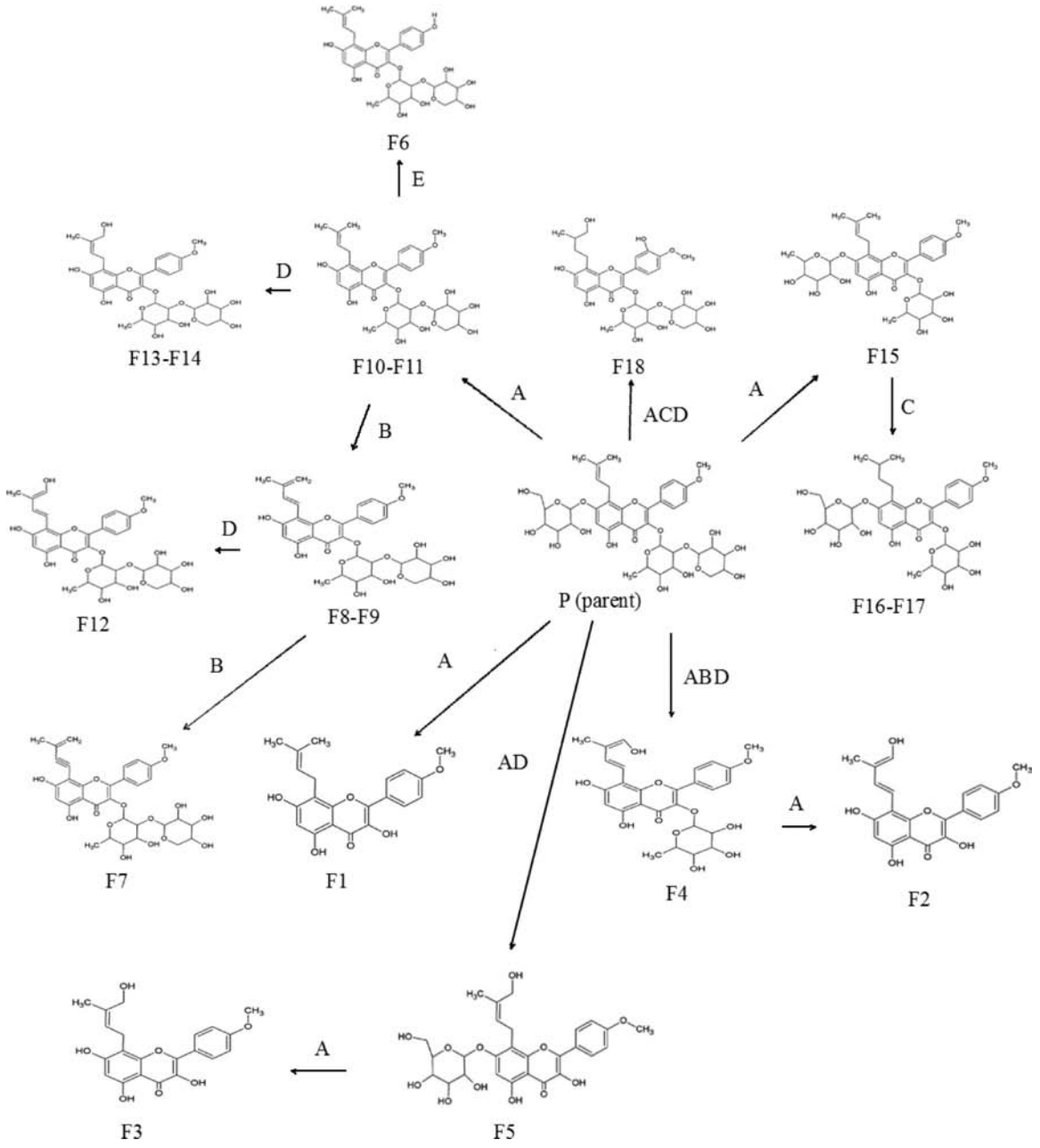

Figure 2. Proposed major metabolic pathway of epimedin B in rat feces: (A) desugarization; (B) dehydrogenation; (C) hydrogenation; (D) hydroxylation; and (E) demethylation.

Table 3. Accurate Mass Measurement for the Protonated Molecules of Metabolites in Rat Bile

no.	formula	t_R (min)	calcd m/z	exptl m/z	mg/L error
P	$C_{38}H_{48}O_{19}$	2.82	809.2790	809.2895	3.4
D1	$C_{32}H_{40}O_{13}$	3.96	633.2469	633.2546	−0.1
D2	$C_{32}H_{40}O_{13}$	4.17	633.2469	633.2558	1.8
D3	$C_{32}H_{38}O_{14}$	4.00	647.2262	647.2336	−0.6
D4	$C_{33}H_{38}O_{16}$	2.92	691.2160	691.2251	1.9
D5	$C_{37}H_{46}O_{19}$	2.28	795.2633	795.2688	−2.9
D6	$C_{38}H_{48}O_{19}$	2.32	809.7333	809.7949	0.4
D7	$C_{38}H_{46}O_{20}$	2.80	823.2582	823.2683	2.7
D8	$C_{39}H_{48}O_{20}$	2.84	837.2739	837.2847	3.6
D9	$C_{44}H_{54}O_{28}$	2.65	1031.2802	1031.2865	−1.4

Table 4. Relative Peak Area of Metabolites in Bile of Different Collection Times[a]

no.	0−4 h	4−8 h	8−12 h
P	120.00	114.60	N/A
D1	N/A	36.80	N/A
D2	39.40	N/A	N/A
D3	17.10	29.40	N/A
D4	N/A	3.00	N/A
D5	94.10	123.80	N/A
D6	N/A	N/A	25.50
D7	124.10	144.70	N/A
D8	N/A	N/A	34.00
D 9	N/A	N/A	5.80

[a]N/A = not available.

dx.doi.org/10.1021/jf304625x | J. Agric. Food Chem. 2013, 61, 3589−3599

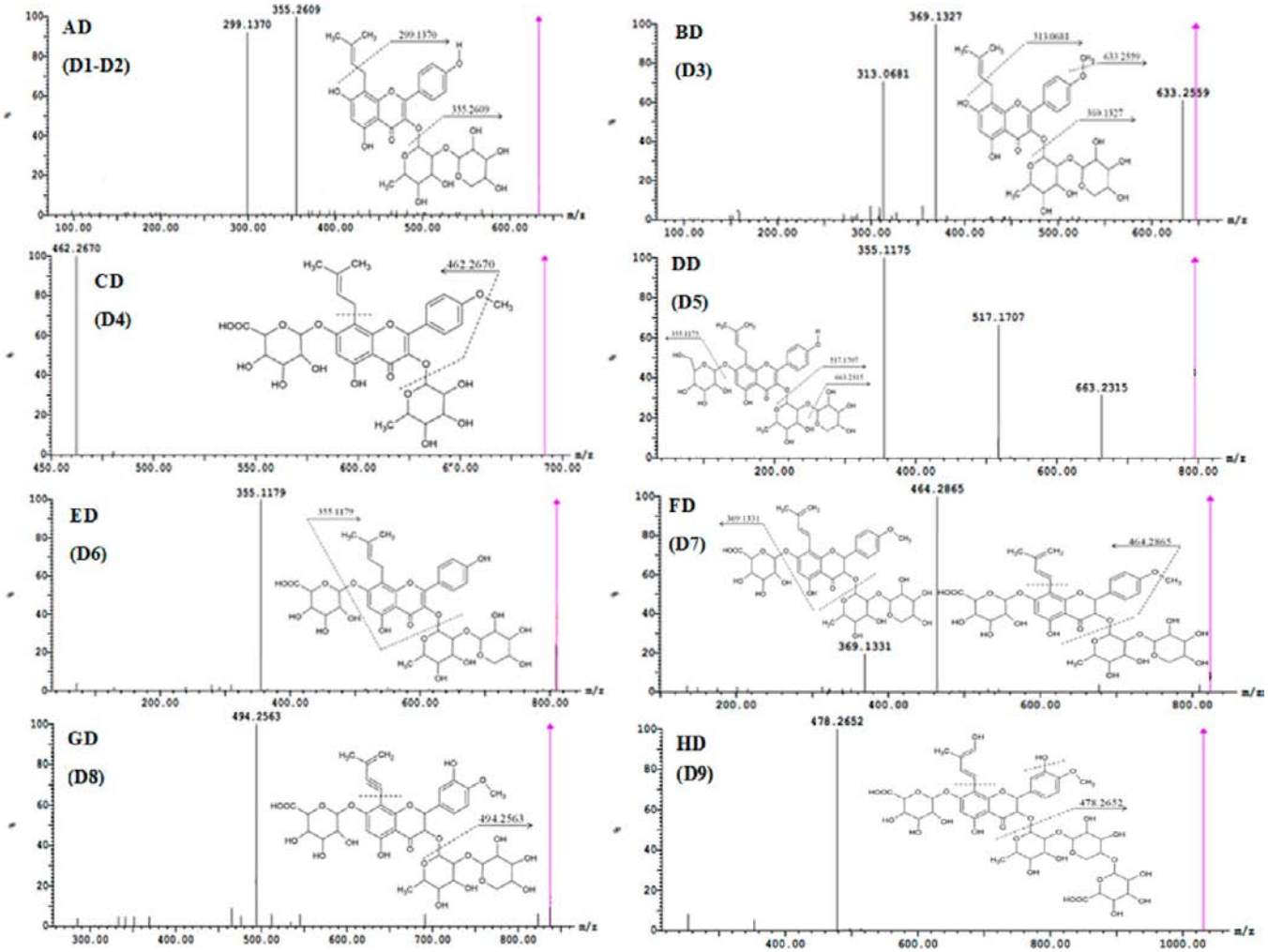

Figure 3. Mass spectra of metabolites of epimedin B in rat bile.

losses of glucose, xylose, and glucose, rhamnose, and xylose from the parent compound (**P**), respectively. These results indicated the ions were the desugarization products of epimedin B.

Therefore, **F10** and **F11** (Figure 1IF) and **F15** (Figure 1LF) were thought to be sagittatoside B and icariin, respectively, formed due to the losses of glucose and xylose at positions 7 of the A ring and 3 of the B ring of epimedin B, respectively. On the other hand, **F1** (Figure 1AF) was thought to be icaritin because of the loss of glucose, rhamnose, and xylose at position 7 of the A ring and position 3 of the B ring of epimedin B.

The molecular ion at *m*/*z* 633.2105 (**F6**) and its product ions at *m*/*z* 355.1173 and 299.0558 (Figure 1FF) were all 14 Da less than *m*/*z* 647.2262 (**F10** and **F11**) and its product ions at *m*/*z* 369.1342 and 313.0700, respectively. Therefore, **F6** was identified as the demethylsagittatoside B, and the demethylation position was at the unique saturated C−O bond at position 4′ of the C ring.

Furthermore, the molecular ion at *m*/*z* 645.2105 (**F8** and **F9**) and its product ion at *m*/*z* 367.1182 (Figure 1HF) were 2 Da less than 647.2262 (**F10** and **F11**) and its product ions at *m*/*z* 369.1342, respectively. Similarly, the molecular ion at *m*/*z* 643.6040 (**F7**) and its product ion at *m*/*z* 365.1002 (Figure 1GF) were all 4 Da less than 647.2262 (**F10** and **F11**) and its product ion at *m*/*z* 369, respectively. Therefore, **F7**−**F9** were identified as the dehydrogenation products of sagittatoside B, and the dehydrogenated position was thought to be at the isopentene group at position 8 of the A ring.

The molecular ion at *m*/*z* 661.2054 (**F12**) was 16 Da more than *m*/*z* 645.2105 (**F8** and **F9**). Hence, **F12** was characterized as the oxidation product of **F8** and **F9**, and the oxidation position was thought to be at the terminal methyl of the isopentene group at position 8 of the A ring. Therefore, **F12** was designated as 1,3-isoprene alcohol sagittatoside B.

The molecular ion at *m*/*z* 663.2211 (**F13** and **F14**) and its product ions at *m*/*z* 385.1265 (Figure 1KF) were all 16 Da more than *m*/*z* 647.2262 (**F10** and **F11**) and its product ion at *m*/*z* 369.1342 (Figure 1IF). Therefore, **F13** and **F14** were characterized as the oxidation products of **F10** and **F11**, and the oxidation position was at the terminal methyl of the isopentene group at position 8 of the A ring. The ion *m*/*z* 367.1149 has been reported to be produced by the McLafferty rearrangement of the isopentene group at position 8 of the A ring.

The molecular ion at *m*/*z* 679.2160 (**F16** and **F17**) was 2 Da more than *m*/*z* 677.2367 (**F15**). Therefore, **F16** and **F17** were identified as the hydrogenation product of icariin, and the hydrogenation position was at the isopentene group at position 8 of the A ring.

The molecular ion at *m*/*z* 681.2316 (**F18**) and its product ion at *m*/*z* 403.1385 (Figure 1NF) were 18 Da more than *m*/*z* 663.2211 (**F13** and **F14**) and its product ion at *m*/*z* 385.1265, respectively. So, **F18** could be characterized as the hydrox-

dx.doi.org/10.1021/jf304625x | J. Agric. Food Chem. 2013, 61, 3589−3599

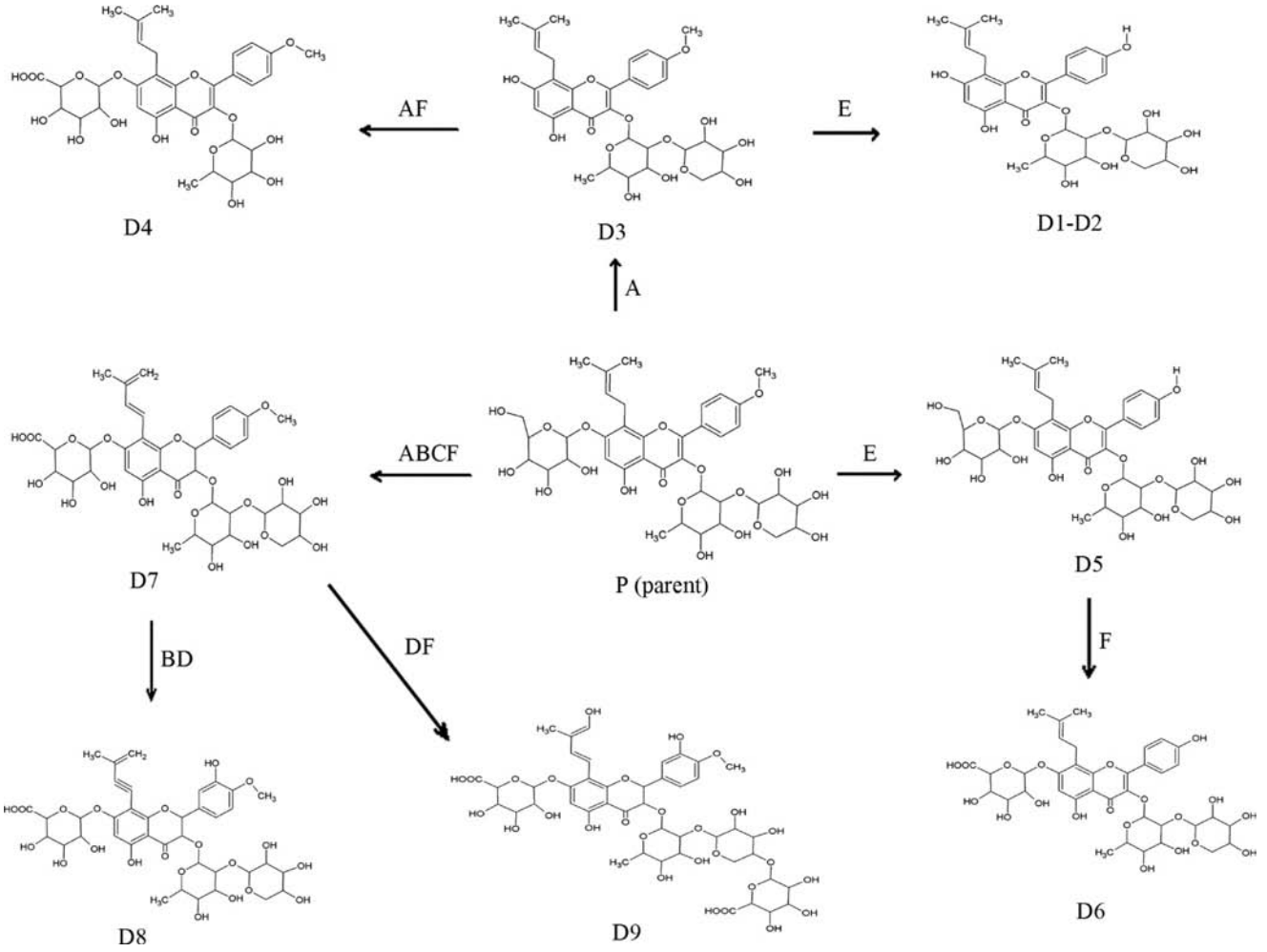

Figure 4. Proposed major metabolic pathway of epimedin B in rat bile: (A) desugarization; (B) dehydrogenation; (C) hydrogenation; (D) hydroxylation; (E) demethylation; and (F) glucuronidation.

Table 5. Accurate Mass Measurement for the Protonated Molecules of Metabolites in Rat Urine

no.	formula	t_R (min)	calcd m/z	exptl m/z	mg/L error
P	$C_{38}H_{48}O_{19}$	2.82	809.2790	809.2895	3.4
N1	$C_{21}H_{20}O_6$	4.50	369.1260	369.1314	1.4
N2	$C_{21}H_{20}O_6$	5.58	369.1260	369.1317	−5.7
N3	$C_{21}H_{18}O_7$	4.88	383.1053	383.1119	−3.0
N4	$C_{21}H_{20}O_7$	4.66	385.1209	385.1281	−1.6
N5	$C_{27}H_{30}O_{13}$	3.42	563.1686	563.1762	−0.4
N6	$C_{32}H_{38}O_{14}$	4.00	647.2262	647.2341	0.2
N7	$C_{32}H_{38}O_{14}$	4.02	647.2340	647.2407	−1.7
N8	$C_{32}H_{36}O_{15}$	3.36	661.2054	661.2137	0.7
N9	$C_{32}H_{38}O_{15}$	3.28	663.2211	663.2318	4.4
N10	$C_{33}H_{40}O_{15}$	3.88	677.2367	677.2460	2.2

Table 6. Relative Peak Area of Metabolites in Urine of Different Collection Times[a]

no.	0−12 h	12−24 h
P	N/A	N/A
N1	9.30	N/A
N2	96.50	138.30
N3	5.90	N/A
N4	2.80	24.10
N5	N/A	3.50
N6	N/A	331.20
N7	N/A	103.20
N8	13.60	7.30
N9	23.50	23.80
N10	N/A	12.60

[a]N/A = not available.

ylation and hydrogenation product of **F13** and **F14**. The hydroxylation position was at position 3′ of the C ring, and the hydrogenation position was also at the isopentene group at position 8 of the A ring.

The molecular ion at m/z 547.1737 (**F5**) was 262 Da less than the 809.2790 (**P**); since the 262 Da product was formed by the reduction of 16 Da from a moiety of 278 Da, **F5** was the oxidation product of icariside I.

Since the molecular ion at m/z 385.1209 (**F3**) was 162 Da less than m/z 547.1737 (**F5**), **F3** was thought to be produced by the loss of glucose at position 7 of the A ring of **F5**. Furthermore, the MS fragmentation patterns of the molecular ions at m/z 355.2624 and m/z 337.2533 are shown in Figure 1CF.

The molecular ion at m/z 529.1632 (**F4**) was 14 Da more than m/z 515 (baohuoside I). So, **F4** could be characterized as oxidation products of baohuoside I, and the oxidation position was at the terminal methyl of isopentene group at position 8 of the A ring, coupled with the migration of the double bond of

dx.doi.org/10.1021/jf304625x | J. Agric. Food Chem. 2013, 61, 3589−3599

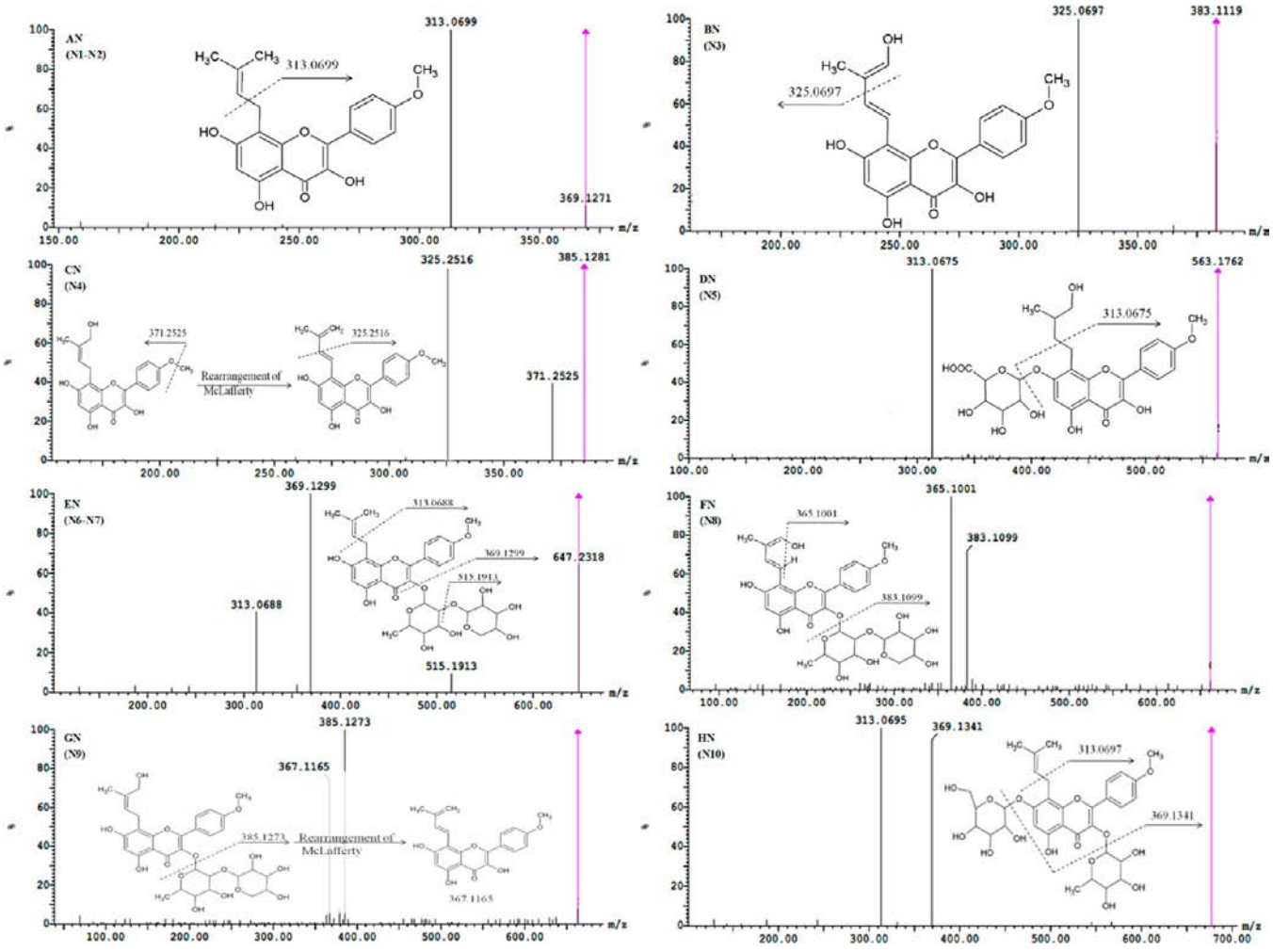

Figure 5. Mass spectra of metabolites of epimedin B in rat urine.

the isopentene group. According to the structure of the baohuoside I, **F4** (Figure 1DF) was designated as 1,3-isoprene alcohol baohuoside I.

The molecular ion at *m*/*z* 383.1053 (**F2**) was produced by the neutral loss of 146 Da corresponding to the loss of rhamnose from *m*/*z* 529.1632 (**F4**). The result suggested that *m*/*z* 383.1053 (**F2**) should be the desugarization product of *m*/*z* 529.1632 (**F4**). Hence, **F2** was called 1,3-isoprene alcohol icaritin.

The trace prototype of epimedin B (**P**, Table 2) was observed in the feces samples, which was probably caused by the administration of high-dose oral epimedin B (80 mg/kg body weight) to rats. This result suggested that the first-pass biotransformation in the alimentary canal had reached a saturation level, since the concentration of epimedin B had exceeded the utmost limit.

Metabolites Detected in the Rat Bile Samples. In all, nine metabolites (**D1**−**D9**) were tentatively identified by MS in the rat bile samples (Table 3). Of these, four, including **D5**−**D7** and **D9**, were to our knowledge, reported for the first time. As stated in the literature, 7-*O*-gluA was the predominant metabolic pathway in the liver,[13] and five of the metabolite profiles in the liver were the glucuronidation products. The relative peak area of the metabolites detected in the bile samples collected at different collection times is shown in Table 4. The TOF-MS spectra of these metabolites and the proposed major metabolic pathway of epimedin B in rat bile are shown in Figures 3 and 4, respectively.

The molecular ions of **D5** (*m*/*z* 795.2633) and **D3** (*m*/*z* 647.2262) were produced by the neutral loss of 14 and 162 Da diagnostic of methyl and glucose from the parent compound, respectively. So **D5** was considered as the demethylation product of the parent compound, and the structure of **D3** has been speculated in the Metabolites Detected in the Rat Feces Samples section. On the basis of the structure of the parent compound, **D5** (Figure 3DD) was called demethylepimedin B.

The molecular ion at *m*/*z* 633.2469 (**D1** and **D2**) and its product ions at *m*/*z* 355.2609 and 299.1370 (Figure 3FF) were all 14 Da less than *m*/*z* 647.2262 (**D3**) and its product ions at *m*/*z* 369.1327 and 313.0681, respectively. Therefore, **D1** and **D2** were also identified as the desmethylsagittatoside B, the same as **F6**. But, their retention times were different, so **F6**, **D1**, and **D2** were considered as isomers.

The molecular ion at *m*/*z* 691.2160 (**D4**) was 44 Da more than *m*/*z* 647.2262 (**D3**). This difference was accounted for by the difference between 176 Da (monoglucuronide) and 132 Da (xylose). For prenylflavonoids, since substitution was more easily possible at the C-7 position than at the C-3 position, gluA was deduced at the C-7 position. According to the structure of the icaritin, **D4** was identified as icaritin-3-*O*-rha-7-*O*-gluA.

The molecular ion at *m*/*z* 809.7333 (**D6**) was equivalent to *m*/*z* 809.2790 (**P**), and the retention time of **D6** was shorter

dx.doi.org/10.1021/jf304625x | J. Agric. Food Chem. 2013, 61, 3589−3599

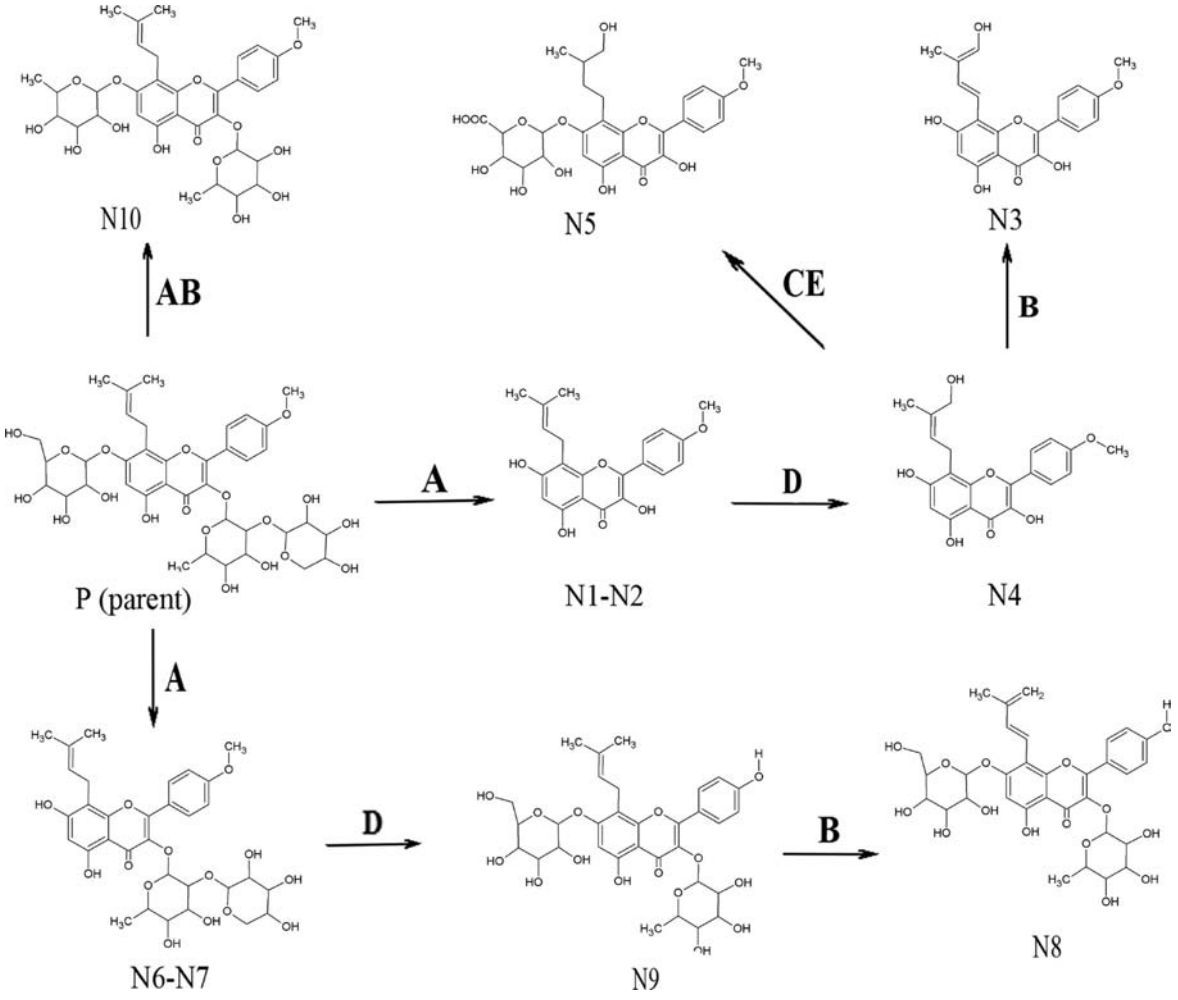

Figure 6. Proposed major metabolic pathway of epimedin B in rat urine: (A) desugarization; (B) dehydrogenation; (C) hydrogenation; (D) hydroxylation; and (E) glucuronidation.

Table 7. Accurate Mass Measurement for the Protonated Molecules of Metabolites in Rat Plasma

no.	formula	t_R (min)	calcd m/z	exptl m/z	mg/L error
P	$C_{38}H_{48}O_{19}$	2.82	809.2790	809.2895	3.4
M1	$C_{21}H_{20}O_6$	5.00	517.5370	517.1725	3.0
M2	$C_{21}H_{18}O_7$	4.04	661.6192	661.2504	1.2
M3	$C_{21}H_{20}O_7$	3.50	665.6079	665.2076	−0.8
M4	$C_{27}H_{28}O_{11}$	2.69	721.6281	721.1993	1.9
M5	$C_{27}H_{30}O_{12}$	2.72	721.6281	721.1969	−1.5
M6	$C_{31}H_{36}O_{14}$	2.74	721.6281	721.1987	1.0

than **P**, so **D6** was conjectured as the glucuronidation product of demethylepimedin B, which should be called demethylepimedin B-7-*O*-gluA.

The molecular ion at m/z 823.2582 (**D7**) was 132 Da more than m/z 691.2160 (**D4**), and the product ion of **D7** at m/z 464.2865 was 2 Da more than that of **D4** at m/z 462.2670. Therefore, **D7** was considered as a flavanone compound.

The molecular ion at m/z 837.2739 (**D8**) was 14 Da more than m/z 823.2582 (**D7**). This accounted for the difference between 16 Da (O) and 2 Da (2 H). Hence, **D8** was considered as the hydroxylation and dehydrogenation product of **D7**.

Table 8. Relative Peak Area of Metabolites in Plasma of Different Collection Times[a]

no.	15 min	30 min	45 min	60 min	90 min	120 min	240 min	420 min	600 min	780 min
P	N/A	N/A	N/A	N/A	N/A	N/A	N/A	N/A	N/A	N/A
M1	3.72	38.20	23.34	N/A	10.23	N/A	13.70	5.70	N/A	1.57
M2	2.14	10.92	N/A	8.83	N/A	9.60	N/A	6.95	N/A	N/A
M3	0.45	N/A	1.24	N/A	0.88	0.90	N/A	N/A	0.47	0.55
M4	1.99	N/A	9.28	N/A	4.23	N/A	5.60	N/A	0.87	N/A
M5	N/A	8.90	6.27	N/A	N/A	3.12	N/A	2.60	N/A	5.30
M6	N/A	N/A	2.20	N/A	0.67	N/A	N/A	1.26	2.09	N/A

[a]N/A = not available.

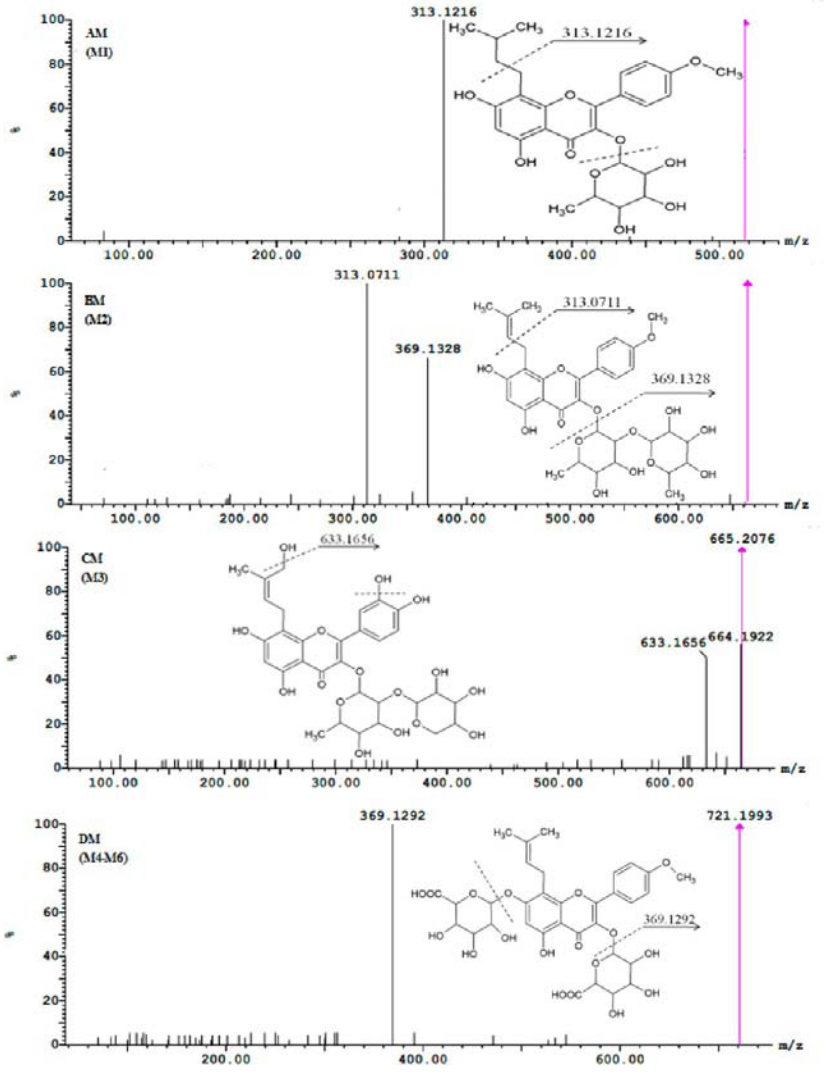

Figure 7. Mass spectra of metabolites of epimedin B in rat plasma.

The molecular ion at m/z 1031.2802 (**D9**) was 208 Da more than m/z 823.2582 (**D7**). This difference was accounted for by the sum of 176 Da (monoglucuronide) and 32 Da (2 O). In addition, one of the oxidation positions was at the terminal methyl of isopentene group at position 8 of the A ring.

Metabolites Found in the Rat Urine Samples. In all, 10 metabolites (**N1**−**N10**) were tentatively characterized by MS in the rat urine (Table 5), and **N5** was to our knowledge reported for the first time. The relative peak area of metabolites detected in the urine samples collected at different times is shown in Table 6. The TOF-MS spectra of these metabolites and the proposed major metabolic pathway of epimedin B in rat urine are shown in Figures 5 and 6.

The structures of the 10 metabolites, except **N5**, have been speculated above. The molecular ion at m/z 563.1686 (**N5**) was 194 Da more than 369.1260 (**N1** and **N2**). The difference accounted for the sum of 176 Da (monoglucuronide), 16 Da (O) and 2 Da (2 H). Besides, the retention time of **N5** was 3.42 min, whereas those of **N1** and **N2** were 4.50 and 5.58 min, respectively. Therefore, **N5** might be the glucuronidation, hydroxylation, and hydrogenation product of **N1** and **N2**.

Metabolites Detected in the Rat Plasma Samples. Six metabolites (**M1**−**M6**) were identified or tentatively characterized by MS in the rat plasma (Table 7). Of these, two, including **M1** and **M3**, were to our knowledge reported for the first time. The relative peak area of the metabolites in the plasma collected at different collection times is shown in Table 8. The TOF-MS spectra of these metabolites and the proposed major metabolic pathway of epimedin B in rat plasma are shown in Figures 7 and 8, respectively.

The molecular ion at m/z 517.5370 (**M1**) was 2 Da more than m/z 515 (baohuoside I). So, **M1** could be characterized as the hydrogenation product of baohuoside I, and the hydrogenation position was thought to be at the double bond of the isopentene group at position 8 of the A ring.

The molecular ion at m/z 661.6192 (**M2**) was 292 Da more than m/z 369 (icaritin). Therefore, **M2** was produced by the glycosylation of two rhamnose units from icaritin. According to the structure of icaritin, **M2** (Figure 6BM) was called icaritin-3-*O*-rha-rha.

The produced ion at m/z 633.1656 was 32 Da less than its parent molecular ion at m/z 665.6079 (**M3**), and the 633 ion has been speculated above. Hence, **M3** was considered as the double oxidation product of **F6** (633.2105).

The molecular ion at m/z 721.6281 (**M4**−**M6**) was 352 Da more than icaritin, which was the diglucuronide conjugation of icaritin. According to the structure of the icaritin, **M4**−**M6** (Figure 7DM) were called icaritin-3-*O*-gluA-7-*O*-gluA.

dx.doi.org/10.1021/jf304625x | *J. Agric. Food Chem.* 2013, 61, 3589−3599

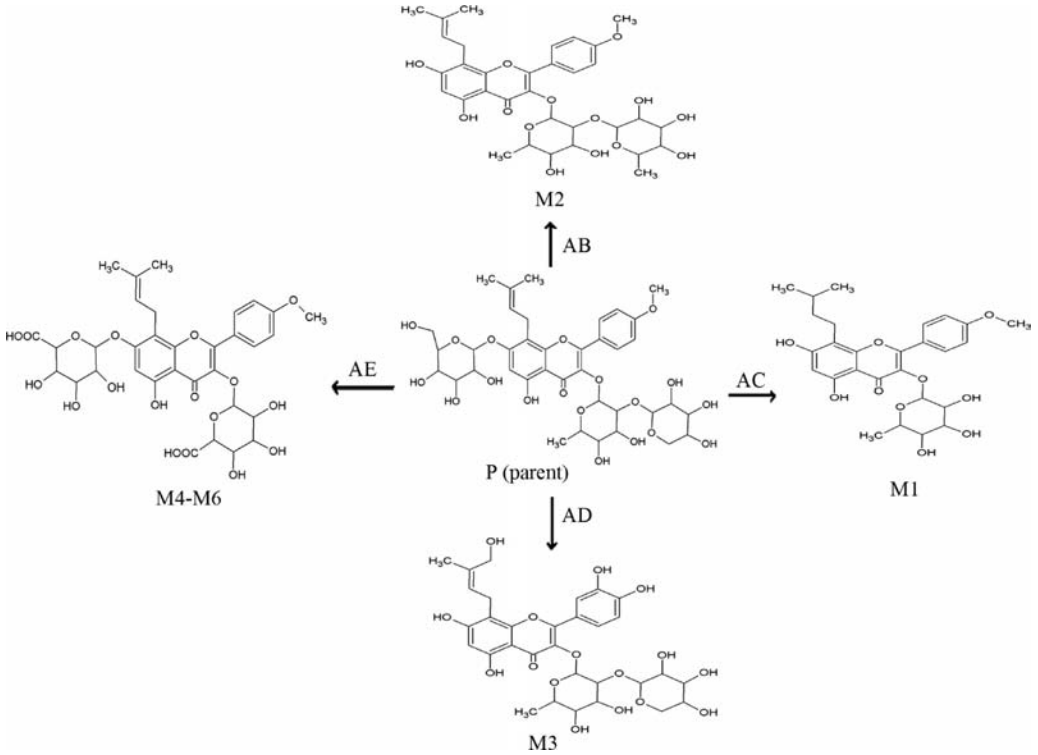

Figure 8. Proposed major metabolic pathway of epimedin B in rat plasma: (A) desugarization; (B) glycosylation; (C) hydrogenation; (D) hydroxylation; and (E) glucuronidation.

Double peaks have been reported to appear in the plasma concentration−time curves in rats orally administrated epimedin B.[14] This suggests the role of hepato-enteral circulation in the excretion of epimedin B. When the commom points between **M4−M6** were analyzed, the diglucuronic acid conjugation react was found to affect the enterohepatic circulation of epimedin B.

The circulation level reached in plasma after the oral administration of epimedin B was low, which was probably related to its limited absorption.[15,16] In general, the absorption of epimedin B in the digestive tract starts in the ileum, where more complex structures (glycosides) that cannot be absorbed in its native form are hydrolyzed by intestinal enzymes or the colonic microflora before they can be absorbed.[17] The hydrolyzed metabolites of epimedin B are easily diffused and absorbed in intestine. Among the detected metabolites, 14 of the 18 metabolites found in the feces samples, 8 of the 9 metabolites in the bile samples, 9 of the 10 metabolites in the urine samples, and all of the plasma metabolites were the hydrolysis products of epimedin B. Furthermore, most of the metabolites were the products of partial hydrolysis of 7-*O*-glucosides. The products of phase II metabolites were excreted from the bile and urine in the form of mono- and diglucuronic acid conjugations. The difference in the number of metabolite products between urinary and biliary excretions illustrated that epimedin B was mostly excreted from the bile in rats; this finding was consistent with the literature.[12]

AUTHOR INFORMATION

Corresponding Author

*E-mail: xiaobinjia_nj@126.com; phone/fax: +86 25 85637809.

Funding Sources

This work was supported by the Natural Science Foundation of China (nos. 30572372, 30973944, 81274088, and 30973978), the science and technology project fund of Jiangsu Province Bureau of Traditional Chinese Medicine (no. LZ09067), and the foundation for high-level talent on six areas of Jiangsu province (no. HZ09032).

Notes

The authors declare no competing financial interest.

ABBREVIATIONS USED

UPLC/Q-TOF-MS, ultraperformance liquid chromatography coupled to quadrupole-time-of-flight mass spectrometry; CE, capillary electrophoresis; GC, gas chromatography; LC, liquid chromatography; PE-10, polyethylene 10; ESI, electrospray ionization; E_c, collision energy; gluA, glucuronidation

REFERENCES

(1) Wu, Y. T.; Lin, C. W.; Lin, L. C.; Chiu, A. W.; Chen, K. K.; Tsai, T. H. Analysis of Biliary Excretion of Icariin in Rats. *J. Agric. Food Chem.* **2010**, *58*, 9905−9911.

(2) Meng, F. H.; Li, Y. B.; Xiong, Z. L.; Jiang, Z. M.; Li, F. M. Osteoblastic proliferative activity of *Epimedium brevicornum* Maxim. *Phytomedicine* **2005**, *12*, 189−193.

(3) Wang, Y. K.; Huang, Z. Q. Protective Effects of Icariin on Human Umbilical Vein Endothelial Cell Injury Induced by H_2O_2 in Vitro. *Pharmacol. Res.* **2005**, *52*, 174−182.

(4) An, D. N.; Victoria, P.; Stuart, M.; Denis, D. K. Estrogenic Activity of a Polyphenolic Extract of the Leaves of *Epimedium brevicornum*. *Fitoterapia* **2005**, *76*, 35−40.

(5) Zhang, H. F.; Yang, T. S.; Li, Z. Z.; Wang, Y. Simultaneous Extraction of Epimedin A, B, C and Icariin from Herba Epimedii by Ultrasonic Technique. *Ultrason. Sonochem.* **2008**, *15*, 376−385.

(6) Chen, Y.; Zhao, Y. H.; Jia, X. B.; Hu, M. Intestinal Absorption Mechanisms of Prenylated Flavonoids Present in the Heat-Processed

Epimedium koreanum Nakai (Yin Yanghuo). *Pharm. Res.* **2008**, *25*, 2190−2199.
(7) Fu, M. L.; Wang, W.; Chen, F.; Dong, Y. C.; Liu, X. J.; Ni, H.; Chen, Q. H. Production of 8-Prenylnaringenin from Isoxanthohumol through Biotransformation by Fungi Cells. *J. Agric. Food Chem.* **2011**, *59*, 7419−7426.
(8) Li, Y. B.; Xiong, Z. L.; Li, F. M. Determination of Epimedin C in Rat Plasma by Reversed-Phase High-Performance Chromatography after Oral Administration of Herba Epimedii Extract. *J. Chromatogr., B* **2005**, *821*, 235−239.
(9) Shen, P.; Wong, S. P.; Yong, E. L. Sensitive and Rapid Method to Quantify Icaritin and Desmethylicaritin in Human Serum Using Gas Chromatography−Mass Spectrometry. *J. Chromatogr., B* **2007**, *857*, 47−52.
(10) Zhao, H. Y.; Fan, M. X.; Fan, L.; Sun, J. H.; Guo, D. A. Liquid Chromatography−Tandem Mass Spectrometry Analysis of Metabolites in Rats after Administration of Prenylflavonoids from Epimediums. *J. Chromatogr., B* **2010**, *878*, 1113−1124.
(11) Qian, Q.; Li, S. L.; Sun, E.; Zhang, K. R.; Tan, X. B.; Wei, Y. J.; Fan, H. W.; Cui, L.; Jia, X. B. Metabolite Profiles of Icariin in Rat Plasma by Ultra-fast Liquid Chromatography Coupled to Triple-Quadrupole/Time-of-Flight Mass Spectrometry. *J. Pharm. Biomed. Anal.* **2012**, *66*, 392−398.
(12) Zhao, H. Y.; Sun, J. H.; Fan, M. X.; Fan, L.; Zhou, L.; Li, Z.; Han, J.; Wang, B. R.; Guo, D. A. Analysis of Phenolic Compounds in Epimediumplants Using Liquid Chromatography Coupled with Electrospray Ionization Mass Spectrometry. *J. Chromatogr., A* **2008**, *1190*, 157−181.
(13) Andrea, J. D.; Bao, Y. P.; Morgan, M. R. A.; Gary, W. Conjugation Position of Quercetin Glucuronides and Effect on Biological Activity. *Free Radical Biol. Med.* **2000**, *29*, 1234−1243.
(14) Wu, C. S.; Zhang, J. L.; Zhou, T. H.; Guo, B. L.; Wang, Y. L.; Hou, J. F. Simultaneous Determination of Seven Flavonoids in Dog Plasma by Ultra-performance Liquid Chromatography−Tandem Mass Spectrometry and Its Application to a Bioequivalence Study of Bioactive Components in Herba Epimedii and Er-Xian Decoction. *J. Pharm. Biomed. Anal.* **2011**, *54*, 186−191.
(15) Aura, A. Microbial Metabolism of Dietary Phenolic Compounds in the Colon. *Phytochem. Rev.* **2008**, *7*, 407−429.
(16) Chen, Y.; Zhao, Y. H.; Jia, X. B.; Hu, M. Intestinal Absorption Mechanisms of Prenylated Flavonoids Present in the Heat-Processed Epimedium koreanum Nakai (Yin Yanghuo). *Pharm. Res.* **2008**, *25*, 2190−2199.
(17) Aida, S.; Alba, M.; Romero, M. P.; Jordi, R.; Nadia, O.; Motilva, M. J. Metabolic Pathways of the Colonic Metabolism of Flavonoids (Flavonols, Flavones and Flavanones) and Phenolic Acids. *Food Chem.* **2012**, *130*, 383−393.